

## Effect of Fungal Infection with *Bipolaris sorokiniana* on Photosynthetic Light Reactions in Wheat Analyzed by Fluorescence Spectroscopy

D. N. Matorin<sup>a,\*</sup>, N. P. Timofeev<sup>b</sup>, A. P. Glinushkin<sup>c</sup>, L. B. Bratkovskaya<sup>b</sup>, and B. K. Zayadan<sup>d</sup>

<sup>a</sup> Department of Biophysics, Faculty of Biology, Moscow State University, Moscow, 119234 Russia

<sup>b</sup> Department of Hydrobiology, Faculty of Biology, Moscow State University, Moscow, 119234 Russia

<sup>c</sup> All-Russia Research Institute of Phytopathology, Bolshie Vyazemy, 143050 Russia

<sup>d</sup> Al-Farabi Kazakh State University, Almaty, 050040 Republic of Kazakhstan

\*e-mail: matorin@biophys.msu.ru

Received July 8, 2018; in final form, September 15, 2018

**Abstract**—Common root rot is a widespread cereal disease caused by a plant pathogenic fungus *Bipolaris sorokiniana*. The influence of fungal infection on photosynthetic light reactions in soft wheat has been studied by a simultaneous registration of fast and delayed chlorophyll fluorescence induction curves as well as the redox state of a P700 pigment. In the case of infected plants, the reduction of a quantum yield of electron transport in the photosystem II ( $\phi E_0$ ) and performance index on absorption basis ( $PI_{ABS}$ ), as well as the increase of energy dissipation per a reaction center ( $DI_0/RC$ ) and  $\Delta pH$ -dependent nonphotochemical fluorescence quenching ( $qE$ ), has been observed. A reduction of the induction peak of delayed chlorophyll fluorescence at 10–50 ms has been revealed. Reactions of the photosystem I show a greater resistance to fungal infection as compared with photosystem II. Parameters of chlorophyll *a* fluorescence induction may be used for the early diagnostics of pathogen-induced changes in the physiological state of plants.

**Keywords:** *Triticum aestivum* L., *Bipolaris sorokiniana* Shoemaker, photosystem I and II, chlorophyll fluorescence, photosynthesis, M-PEA-2.

**DOI:** 10.3103/S0096392518040065

### INTRODUCTION

Common or helminthosporium-induced root rot is a widespread disease caused by a plant pathogenic fungus *Bipolaris sorokiniana*, which infects wheat, rye, barley, oat, and some other cereal plants [1]. Cytological and molecular mechanisms of interaction between the pathogen and a host plant are well-known, which makes it possible to use *B. sorokiniana* as a model object for the study of a plant response to the fungal infection [2].

Photosynthesis is one of the stress-sensitive processes occurring within plant cells [3, 4]. Registration of a chlorophyll *a* fluorescence is a promising method to study the response of a plant photosynthetic apparatus to infection with various pathogens [5–9]. This noninvasive method allows a user to obtain a lot of information about the photosynthetic efficiency and the integrity of a photosynthetic apparatus even at the very early stages of leaf pathology.

To date, there are many studies devoted to the effect of fungal pathogens on fluorescence parameters of plant leaves [8–12]. Results of these studies significantly differ, which may be explained by a strong

dependence of plant responses on the state of both plant and fungal parasites as well as on the environmental conditions during disease development. In addition, infection distribution across plant organs is not uniform, which results in a heterogeneity of fluorescence parameters in infected tissues; those organs that are not directly infected may be indirectly modified by a parasite [8, 13]. Nevertheless, chlorophyll *a* fluorescence measurement provides information about the disease character and the level of plant resistance or susceptibility to a specific fungal strain already in the first days of infection. In recent years, analysis of fluorescence induction curves with high time resolution (10  $\mu$ s and higher) is widely used to assess the efficiency of the photosynthetic apparatus of higher plants and algal cultures [3, 4, 14, 15]. The M-PEA-2 fluorimeter used in our studies provides a possibility to measure not only chlorophyll fluorescence but also modulated light reflection at 820 nm, which makes it possible to evaluate the redox state of a P700 pigment of the reaction center ( $RC^1$ ) of the photosystem I (PSI). Thus, the device provides a simultaneous observation of certain PSI and PSII reactions

and also registration of the induced changes in delayed fluorescence [3, 15]. As far as we know, such simultaneous registration of different fluorescence parameters and the P700 redox state during fungal infection of plants has not been performed previously.

The objective of the present study was to assess the effect of infection with a plant pathogenic fungus *Bipolaris sorokiniana* Shoemaker on the parameters of fast and delayed fluorescence induction and on the redox state of RC PSI in soft wheat. The research was focused on determination of infection-sensitive photosynthesis stages to reveal the parameters that are the most suitable for evaluation of the state of infected plants

## MATERIALS AND METHODS

The objects of study were leaves of soft wheat<sup>1 2</sup> (*Triticum aestivum* L.) infected with *B. sorokiniana*. For inoculation, 100 g of sterilized wheat seeds were soaked for 15 min in 100 mL of a spore suspension (10 g of *B. sorokiniana* spores per 100 mL of water) with a thorough shaking and then dried in gauze sacks for 24 h at room temperature. Then both control and infected seeds were germinated in Petri plates on a 25% Knop's solution at a light intensity of  $30 \mu\text{E m}^{-2} \text{s}^{-1}$ .

Fluorescence parameters and a P700 redox state were measured with a M-PEA-2 multifunction plant efficiency analyzer (Hansatech Instruments, United Kingdom) [3, 4, 14, 15] starting from the sixth day of seed germination. Measurements were carried out on intact leaves using a special clip with light fibers providing both light sources and sensors. Prior to measurements, leaves were adapted to the dark for 15 min. Fast and delayed fluorescence was registered via alteration of red light ( $625 \text{ nm}$ ,  $1300 \mu\text{E m}^{-2} \text{s}^{-1}$ ) and short-duration dark intervals sufficient for registration of delayed fluorescence (DF). The DF dynamics reflected changes in the fluorescence intensity within a range of  $0.1\text{--}0.9 \text{ ms}$  between the exciting light pulses. Fluorescence induction kinetics was assessed with the maximum time resolution of  $0.02 \text{ ms}$ . It is considered that changes in the absorption at  $820 \text{ nm}$  reflect the redox state of P700 in the RC of PSI. The intensity of modulated light ( $820 \pm 25 \text{ nm}$ ) was  $1000 \mu\text{E m}^{-2} \text{s}^{-1}$ . The obtained reflection data were normalized to the value obtained at  $t = 0.7 \text{ ms}$  ( $\text{MR}_0$ ) [3]. Characteristics and the protocol of measurements using a M-PEA-2 fluorimeter were described in detail earlier [3, 4, 14, 15].

A quantitative analysis of characteristics of primary photosynthetic processes based on induction curves was carried out using the so-called JIP test [4]. This

test uses the following parameters of kinetic fluorescence induction curves: fluorescence at the light exposure duration of  $20 (F_0)$ ,  $2 (F_J)$ ,  $30 (F_I)$ , and  $6 (F_{6s}) \text{ ms}$ ; maximum fluorescence intensity ( $F_M$ ); and the averaged initial slope of the relative variable chlorophyll *a* fluorescence ( $M_0, \text{ms}^{-1}$ ).

The above-mentioned parameters were used to calculate the following indices:

(1)  $F_V/F_M$  or the maximum quantum yield of a primary photochemical reaction in open RCs of PSII ( $F_V/F_M = (F_M - F_0)/F_M$ );

(2)  $V_J$  or the relative amplitude of the O-J phase, which starts after  $2 \text{ ms}$  of illumination. This index reflects the number of "closed" RCs in relation to the total number of RCs that may be closed ( $V_J = (F_J - F_0)/(F_M - F_0)$ );

(3)  $V_I$  or the relative amplitude of the O-I phase, which starts after  $30 \text{ ms}$  of illumination. This index reflects the capability of PSI and its acceptors to oxidize the plastoquinone pool ( $V_I = (F_I - F_0)/(F_M - F_0)$ );

(4)  $\phi E_0$  or the quantum yield of the electron transfer outside  $Q_A$  at  $t = 0$  ( $\phi E_0 = (1 - V_J)/(F_V/F_M)$ );

(5) ABS/RC or the energy flow absorbed by one active RC. This index reflects the ratio between the number of chlorophyll *a* molecules in antenna complexes radiating fluorescence and the number of active RCs ( $\text{ABS/RC} = (M_0/V_J)/[(F_M - F_0)/F_M]$ );

(6)  $\text{DI}_0/\text{RC}$  or the total amount of energy dissipated by one RC in the form of heat ( $\text{DI}_0/\text{RC} = (\text{ABS/RC}) - M_0(1/V_J)$ );

(7)  $\text{PI}_{\text{ABS}}$  or the performance index, which reflects the functional activity of PSII divided by the absorbed energy ( $\text{PI}_{\text{ABS}} = [1 - (F_0/F_M)]/(M_0/V_J)[(F_M - F_0)/F_0][1 - V_J]/V_J$ );

(8)  $qE$  or the capacity to the pH-induced nonphotochemical fluorescence quenching ( $qE = (F_M - F_{6s})/(F_M - F_0)$ ).

The obtained data were statistically treated and analyzed using a Microsoft Excel 2013 (Microsoft Corporation, United States) and Statistica v. 6.0 (StatSoft, Inc., United States) software packages. Statistical hypotheses were examined using a two-sample T test for independent samples ( $p < 0.05$ ). The sample volume for both control and experimental variants was no less than 10 replications.

## RESULTS AND DISCUSSION

In the case of infected plants, no visible changes in the leaf color were observed within the first 12 days of germination. A small bleaching of pigments was registered only after 14 days of germination.

The measurement of the ratio between the chlorophyll *a* fluorescence intensity under light saturation

<sup>1</sup> Abbreviations used in the paper: RC, reaction center; PS II and PS I, photosystems II and I; QA and QB, primary and secondary quinone electron acceptors; PQ, plastoquinone; DF, delayed fluorescence; P700, pigment of the PS I reaction center.

( $F_M$ ) and under low light intensity (ground fluorescence,  $F_O$ ) makes it possible to determine the maximum efficiency of the PSII processes, which is equal to the  $F_V/F_M$  [3, 4]. The  $F_V/F_M$  index is a dimensionless energy characteristic of the photosynthesis similar to the coefficient of performance. We showed that the maximum quantum yield of a primary photochemical reaction ( $F_V/F_M$ ) in control plants is rather high (0.8). In the case of infected plants, a slight reduction of the  $F_V/F_M$  value was observed on the seventh day of germination (Fig. 1). A decrease of the  $F_V/F_M$  value registered after 10–14 days of germination was caused mainly due to the increase of the minimum fluorescence level  $F_O$  (see Table 1). The similar  $F_O$  increase was also observed earlier by other researchers [12].

To provide a detailed evaluation of infection-caused changes in the photosynthetic apparatus, induction parameters of fast and delayed fluorescence, as well as the P700 redox state, were measured using a M-PEA-2 fluorimeter. The resulting fluorescence induction curves obtained on the sixth and 14<sup>th</sup> days of germination are shown in Fig. 2. For control plants, the fluorescence curve corresponded to the curve described by other authors [14, 16]. The kinetics of light-induced fast fluorescence includes several stages known as the OJIP transition [14]. The initial level O corresponds to the chlorophyll *a* fluorescence intensity at the “opened” RC of PSII ( $F_O$ ), i.e., to the completely oxidized  $Q_A$  acceptors. The O-J stage is determined by the light-induced  $Q_A$  reduction, while the further stages mainly reflect a gradual reduction of electron acceptors after  $Q_A$ .

For infected plants, fluorescence induction curves measured on the sixth day of germination were almost the same as those of control plants. A significant

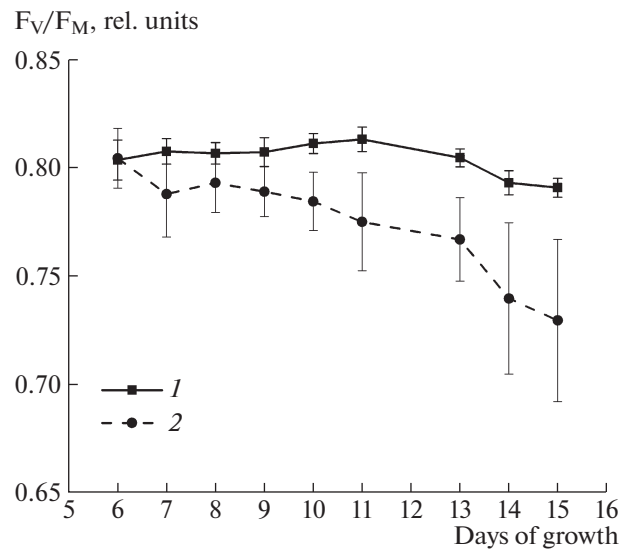


**Fig. 1.** Changes of the maximum quantum yield ( $F_V/F_M$ ) in (1) healthy and (2) infected plants occurring within 6–15 days of germination. The values shown are averaged by ten replications. Confidence intervals ( $p < 0.05$ ) are indicated by vertical bars.

reduction of a variable fluorescence was observed on the subsequent days. Photosynthetic parameters calculated on the basis of the fluorescence induction curve are shown in Table 1.

Along with the  $F_V/F_M$  reduction observed in infected plants, the prolongation of the O-J stage with the corresponding increase of the  $V_J$  index was registered; this fact indicates an increase of the  $Q_B$ -nonreducing RC fraction in PS II [14, 16]. The quantum yield of the PSII electron transport ( $\phi E_0$ ) of infected

**Table 1.** Values of some JIP test parameters, maximum quantum yield ( $F_V/F_M$ ), minimum ( $F_O$ ) and maximum fluorescence ( $F_M$ ), and the relative height of the  $I_1$  and  $I_4$  peaks of delayed fluorescence induction curves of healthy plants (control) and plants infected with root rot measured on the sixth and 14<sup>th</sup> days of infection (% is the percentage of the control value)

	Control	6 <sup>th</sup> day after infection	14 <sup>th</sup> day after infection
$F_V/F_M$	0.8 (100%)	0.8 (100%)	0.74 (92%)*
$F_O$	100%	97%	138%*
$F_M$	100%	97%	104%
$V_J$	0.39 (100%)	0.41 (106%)*	0.44 (113%)*
$V_I$	0.79 (100%)	0.79 (100%)	0.82 (104%)
ABS/RC	3.16 (100%)	3.23 (102%)	3.94 (125%)*
DI <sub>0</sub> /RC	0.62 (100%)	0.65 (102%)	1.09 (175%)*
$\phi E_0$	0.49 (100%)	0.48 (96%)*	0.42 (86%)*
PI <sub>ABS</sub>	2.11 (100%)	1.91 (91%)*	1.52 (72%)*
$qE$	0.24 (100%)	0.25 (104%)	0.30 (125%)*
$I_1$	100%	88%*	77%*

\* Statistically significant difference with the control value ( $p < 0.05$ ).

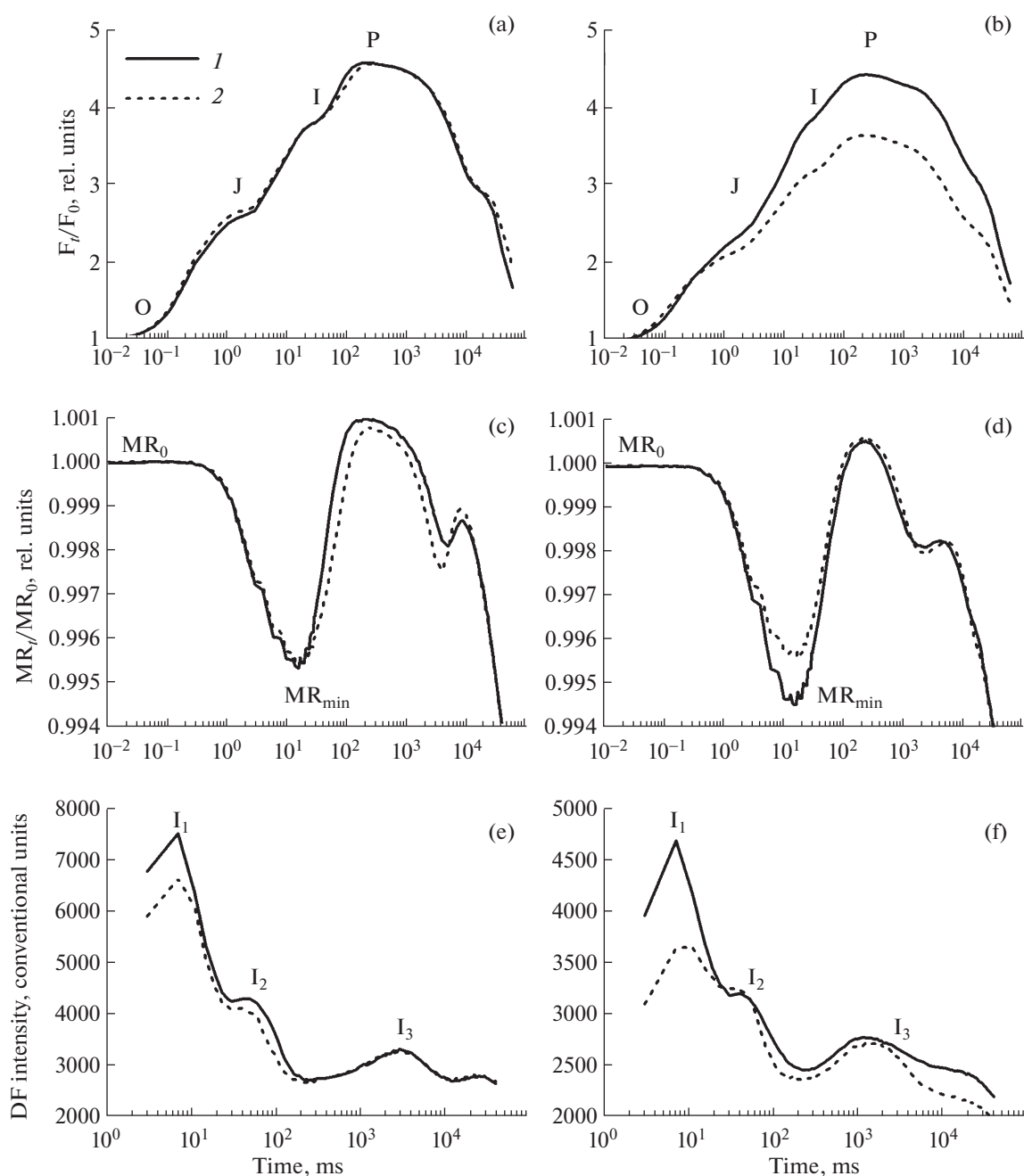


**Fig. 2.** Induction curves of (a, b) fast and (e, f) delayed fluorescence and (c, d) P700 redox state curves of (1) healthy and (2) infected plants. (a, c, e) Left and (b, d, f) right diagrams reflect the state of seedlings on the sixth and 14<sup>th</sup> days, respectively. O, J, I, and P are arbitrary notations of characteristic points of fast fluorescence induction curves used for the JIP test.  $MR_t$ ,  $MR_0$ , and  $MR_{min}$  are the current, initial, and minimal values of the modulated reflection of samples at 820 nm.  $I_1$ ,  $I_2$ , and  $I_3$  indicate characteristic peaks on the delayed fluorescence (DF) induction curve.

plants was also reduced. The O-I stage (3–30 ms) corresponds to the reduction of a plastoquinone (PQ) pool, and the  $V_f$  index is a good indicator of the redox state of a PQ pool in the dark [16]. According to the obtained results, plant infection does not cause changes in this parameter, which indicates that it does not influence on the electron transport at the PQ pool level.

The ABS/RC index (absorption flux per reaction center) in infected plants was increased compared to the control, which is explained by the reduction of active RC fraction. The  $PI_{ABC}$  parameter represents a generalized functional activity index of PCII divided by the amount of absorbed energy (ABS) [3]. The value of this parameter in infected plants was low, which corresponds to a low functional activity of PSII

caused by the reduction of the active PC fraction and activation of nonphotochemical quenching of excited states in pigment antennas. A decrease in the efficiency of excitation energy transfer from the light-harvesting complex to RC should be accompanied with increased dissipation of unused light energy. Actually, the energy dissipation efficiency ( $DI_0/RC$ ) in infected plants is increased compared to the control. This fact corresponds to the increase in a  $\Delta pH$ -dependent nonphotochemical quenching ( $qE$ ) calculated by the fluorescence decrease after the achievement of the maximum value ( $qE = (F_M - F_{6s})/F_V$ ). It is probably caused by the action of helminthosporol, a  $H^+$  ATPase-inhibiting toxin produced by the fungus [17].

The measurement of a modulated reflection at 820 nm showed that the dark-adapted object is characterized by a photoinduced P700 oxidation in PSI RC. The maximum accumulation of oxidized P700<sup>+</sup> reaction centers ( $MR_{min}$ ) was observed at  $t \approx 30$  ms. This accumulation is later replaced by a gradual P700 reduction (Figs. 2c, 2d). During this process, fluorescence signal parameters reflecting the  $Q_A$  reduction go to the plateau almost simultaneously with the P700 reduction processes. A parallel accumulation of reduced forms of P700 and  $Q_A$  reflects the reduction of carriers in the electron transport chain between PSI and PSII due to the lack of the electron outflow from the acceptor part of PSI under conditions of the dark inactivation of ferredoxin-NADP reductase. In the case of long illumination (1–10 s), the second P700 oxidation wave was observed, which can be explained by the electron outflow from the PSI during activation of ferredoxin-NADP reductase and enzymes of the Calvin cycle.

Measurements of the P700 redox state showed a high resistance of PSI to fungal infections. After 6 days, infected leaves demonstrated only a decrease in the reduction rate of RC in PSI compared to that of PSII; this decrease was caused by suppression of non-cyclic electron flow. In the case of a long disease period (14 days), a decrease in the P700 oxidation rate was observed.

Millisecond DF appears as a result of the secondary recombination reaction and depends on the value of the electrochemical proton gradient on a thylakoid membrane; the energy of this gradient reduces activation energy of the recombination reaction [3]. The maximum of the millisecond DF curve ( $I_1$ ) coincides with the growth stage J-I of the fast fluorescence induction curve (Figs. 2e, 2f). Formation of  $I_1$  and  $I_2$  peaks is determined by accumulation of certain redox states of PSII, which are responsible for reverse recombination of charges and emission of DF quanta as well as by the DF enhancement due to electric potential ( $\Delta\psi$ ) formed on the membrane

[3, 14]. The third DF peak ( $I_3$ ) is located in a second range. It is considered to be connected with a

photoinduced formation of a transmembrane proton gradient ( $\Delta pH$ ), which also increases the rate constant of radiation transitions in the RC of PSII.

For leaves of infected plants, the DF intensity on the induction curve is significantly reduced at 10–50 ms ( $I_1$  peak of DF), which is probably caused by a significant reduction of the electric potential on thylakoid membranes. It is significant that changes in the DF intensity are manifested already at the early stages of infection, probably due to a high sensitivity of ATP biosynthesis processes on membranes to fungal toxins.

DF changes in leaves occurring at the early infection stages (incubation period) at the absence of any visible disease manifestations were observed for cotton plants infected with verticillium wilt [18]. Based on the measurement of DF parameters, the authors described three stages for this disease period. During the first 2–7 days, they observed reversible DF changes evidencing the drop of the photosynthesis intensity. This stage probably represents a primary response of the photosynthetic apparatus to the penetration and expansion of the pathogen. The next stage is a false well-being. Finally, significant DF changes occur simultaneously with the appearance of external disease manifestations, which, apparently mean a complete destruction of the photosynthetic apparatus [18]. The analysis of induction curves of healthy and infected cotton plant leaves showed that a partial dissociation of photophosphorylation occurs 3–5 days after infection [18].

We also previously described the DF change caused by the addition of tentoxin, a fungal metabolite disturbing the functioning of  $H^+$  ATPase [19].

Based on the obtained data, we can recommend the use of the  $PI_{ABS}$  (fluorescence induction parameter) and DF induction parameter at 10–50 ms for the early diagnostics of the plant state. Methods used for evaluation of these parameters are noninvasive and simple and can be used to study changes in the photosynthetic apparatus of wheat seedlings infected with plant pathogenic fungi, which occur prior any visible disease manifestations.

## COMPLIANCE WITH ETHICAL STANDARDS

The authors declare that they have no conflict of interest. This article does not contain any studies involving animals or human participants performed by any of the authors.

## REFERENCES

1. Bakonyi, J., Apony, I., and Fisch, G., Diseases caused by *Bipolaris sorokiniana* and *Drechslera tritici-repentis* in Hungary, in *Helminthosporium Blights of Wheat: Spot Blotch and Tan Spot*, Duveiller, E., Dubin, H.J., and Reeves, J., Eds., Mexico City: CIMMYT, 1997, pp. 80–85.

2. Kumar, J., Schäfer, P., Hückelhoven, R., Langen, G., Baltruscha, H., Stein, E., and Kogel, K.H., *Bipolaris sorokiniana*, a cereal pathogen of global concern: Cytological and molecular approaches towards better control, *Mol. Plant Pathol.*, 2002, vol. 3, no. 4, pp. 185–195.
3. Gol'tsev, V.N., Kaladzhi, M.Kh., Kuzmanova, M.A., and Allakhverdiev, S.I., *Peremennaya i zamedlennaya fluorestsentsiya khlorofilla a—teoreticheskie osnovy i prakticheskoe prilozhenie v issledovanii rastenii* (Variable and Delayed Fluorescence of Chlorophyll *a*: Theoretical Foundations and Practical Application in Plant Studies), Moscow—Izhevsk: IKI-RKhD, 2014.
4. Matorin, D.N. and Rubin, A.B., *Fluorestsentsiya khlorofilla vysshikh rastenii i vodoroslei* (Chlorophyll Fluorescence of Higher Plants and Algae), Moscow—Izhevsk: IKI-RKhD, 2012.
5. Christov, I., Stefanov, D., Velinov, T., Goltsev, V., Georgieva, K., Abracheva, P., Genova, Y., and Christov, N., The symptomless leaf infection with grapevine leafroll associated virus 3 in grown in vitro plants as a simple model system for investigation of viral effects on photosynthesis, *J. Plant Physiol.*, 2007, vol. 164, no. 9, pp. 1124–1133.
6. Granum, E., Pérez-Bueno, M., Calderón, C.E., Ramos, C., Vicente, A., Cazorla, F.M., and Barón, M., Metabolic responses of avocado plants to stress induced by *Rosellinia necatrix* analysed by fluorescence and thermal imaging, *Eur. J. Plant Pathol.*, 2015, vol. 142, no. 3, pp. 625–632.
7. Rai, M.K., Shende, S., and Strasser, R.J., JIP test for fast fluorescence transients as a rapid and sensitive technique in assessing the effectiveness of arbuscular mycorrhizal fungi in *Zea mays*: Analysis of chlorophyll *a* fluorescence, *Plant Biosyst.*, 2008, vol. 142, no. 2, pp. 191–198.
8. Scholes, J.D. and Rolfe, S.A., Photosynthesis in localised regions of oat leaves infected with crown rust (*Puccinia coronata*): Quantitative imaging of chlorophyll fluorescence, *Planta*, 1996, vol. 199, no. 4, pp. 573–582.
9. Yan, K., Han, G., Ren, C., Zhao, S., Wu, X., and Bian, T., *Fusarium solani* infection depressed photosystem performance by inducing foliage wilting in apple seedlings, *Front. Plant Sci.*, 2018, vol. 9, p. 479.
10. Scholes, J.D. and Farrar, J.F., Increased rates of photosynthesis in localized regions of a barley leaf infected with brown rust, *New Phytol.*, 1986, vol. 104, no. 4, pp. 601–612.
11. Bassanezi, R.B., Amorim, L., Filho, A.B., and Berger, R.D., Gas exchange and emission of chlorophyll fluorescence during the monocycle of rust, angular leaf spot and anthracnose on bean leaves as a function of their trophic characteristics, *J. Phytopathol.*, 2002, vol. 150, no. 1, pp. 37–47.
12. Kuckenberger, J., Tartachnyk, I., and Noga, G., Temporal and spatial changes of chlorophyll fluorescence as a basis for early and precise detection of leaf rust and powdery mildew infections in wheat leaves, *Precis. Agric.*, 2009, vol. 10, no. 1, pp. 34–44.
13. Tartachnyk, I.I., Rademacher, I., and Kühbauch, W., Distinguishing nitrogen deficiency and fungal infection of winter wheat by laser-induced fluorescence, *Precis. Agric.*, 2006, vol. 7, no. 4, pp. 281–293.
14. Strasser, R.J., Tsimilli-Michael, M., Qiang, S., and Goltsev, V., Simultaneous in vivo recording of prompt and delayed fluorescence and 820-nm reflection changes during drying and after rehydration of the resurrection plant *Haberlea rhodopensis*, *BBA-Bioenergetics*, 2010, vol. 1797, nos. 6–7, pp. 1313–1326.
15. Bulychev, A.A., Osipov, V.A., Matorin, D.N., and Vredenberg, W.J., Effects of far-red light on fluorescence induction in infiltrated pea leaves under diminished  $\Delta pH$  and  $\Delta\phi$  components of the proton motive force, *J. Bioenerg. Biomembr.*, 2013, vol. 45, nos. 1–2, pp. 37–45.
16. Lazár, D. and Schansker, G., Models of chlorophyll *a* fluorescence transients, *Photosynthesis in silico*, Laisk, A., Nedbal, L., and Govindjee, Eds., Dordrecht: Springer, 2009, pp. 85–123.
17. Briquet, M., Vilre, D., Goblet, P., Mesa, M., and Elo, M.C., Plant cell membranes as biochemical targets of the phytotoxin helminthosporol, *J. Bioenerg. Biomembr.*, 1998, vol. 30, no. 3, pp. 285–295.
18. Veselovskii, V.A. and Veselova, T.V., *Lyuminescentsiya rastenii. Teoreticheskie i prakticheskie aspekty* (Luminescence in Plants. Theoretical and Practical Aspects), Moscow: Nauka, 1990.
19. Chamorovskii, S.K. and Matorin, D.N., The effect of calmodulin antagonists on the delayed fluorescence of chloroplasts and algae, *Biokhimiya*, 1984, vol. 49, no. 13, pp. 2029–2034.

Translated by N. Statsyuk

SPELL: 1. Triticum, 2. aestivum